

INFLUENCE OF CUTTING SPEED ON INTENSITY OF THE PLASTIC DEFORMATION DURING HARD CUTTING

VPLIV HITROSTI REZANJA NA INTENZITETO PLASTIČNE DEFORMACIJE MED ODREZOVANJEM

Miroslav Neslušan¹, Ivan Mrkvica², Robert Čep², Mária Čilliková¹

¹University of Žilina, Faculty of Mechanical Engineering, Žilina, Slovakia

²VŠB-Technical University of Ostrava, Ostrava, Czech Republic
miroslav.neslusan@fstroj.utc.sk, robert.cep@vsb.cz

Prejem rokopisa – received: 2013-01-29; sprejem za objavo – accepted for publication: 2013-03-27

The paper deals with an analysis of deformation processes and the aspects related to a chip formation such as the chip thickness, the chip ratio, the shear angle and the chip segmentation during turning the hardened steel 100Cr6. This paper investigates the influence of the cutting speed through a metallographic analysis, a calculation of significant aspects of deformation processes and the resulting experimental study. This experimental study is based on an application of acoustic emission. The results of this study indicate that the cutting speed significantly affects the parameters such as the chip ratio, deformation angle or the speeds in the cutting zone. On the other hand, the experimental study allows an analysis of the specific characters of deformation processes and their real intensity.

Keywords: turning, hardened steel, chip segmentation, acoustic emission

Članek obravnava analizo deformacijskih procesov in vidike pri nastanku odrezka, kot so debelina odrezka, odvzem, rezalni kot in segmentacija odrezkov med struženjem kaljenega jekla 100Cr6. V članku je obravnavan vpliv hitrosti odrezovanja z metalografsko analizo, izračun pomembnih vidikov deformacijskih procesov in temu sledeča eksperimentalna študija. Le-ta temelji na uporabi akustične emisije. Rezultati te študije kažejo pomemben vpliv hitrosti rezanja na parametre, kot so odvzem, deformacije in hitrosti v coni rezanja. Po drugi strani eksperimentalna študija omogoča analizo posebnosti deformacijskih procesov in njihove realne intenzivnosti.

Ključne besede: struženje, kaljeno jeklo, segmentacija ostružkov, akustična emisija

1 INTRODUCTION

With the development of super-hard cutting materials such as ceramics, CBN, PCBN and PCD, etc., the technology of hard turning has attracted considerable interest from several leading manufacturers. In order to specify the potential of this new production technology, several issues of hard turning such as cutting mechanism, tool wear, machined surface integrity, etc., have been recently investigated.^{1,2} One of the significant observations during hard turning, which is different from machining ductile materials, is that consistently cyclic, segmented chips are produced, essentially without any deformation at the shear plane.³⁻⁵

In metal cutting, the principal chip morphologies classified by Komanduri and Brown,⁶ are continuous, serrated chips. In machining, hard and difficult-to-machine materials tend to localize the heat generated due to the strain localization in a narrow band called an adiabatic shear band represented in **Figures 1** and **2**. Adiabatic shear banding investigated by Recht³ is used to describe a localization phenomenon that occurs in the high-strain-rate plastic-deformation processes such as cutting. This phenomenon can be explained in the following way: during a deformation the rate of heat generation is determined by the strain rate, and the heat-

dissipation rate is controlled by the heat conductivity of the material. When the heat-generation rate is larger than the heat-dissipation rate, the temperature increases and the softening associated with such temperature increases as well, exceeding the strain hardening and the catastrophic propagation of the shear occurs. Thermoplastic instability is a significant phenomenon in the segmented chip formation. The thermoplastic instability is caused by a decrease in the flow stress due to the thermal softening associated with an increase in the strain, offsetting

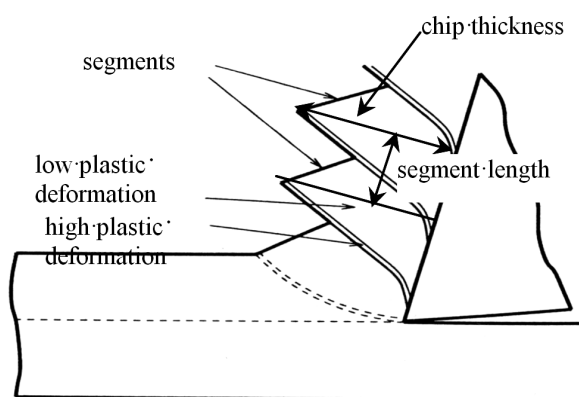


Figure 1: Illustration of a chip formation during hard turning
Slika 1: Prikaz nastanka odrezka pri struženju

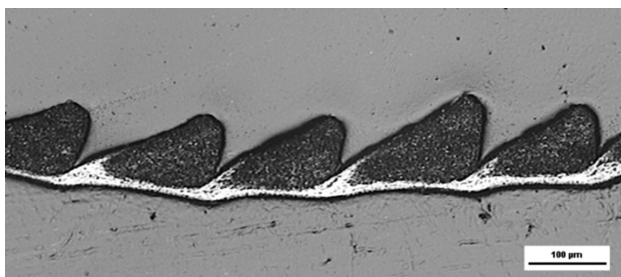


Figure 2: Chips after turning the 100Cr6 (hardened, 62 HRC), SEM, $v_c = 100 \text{ m min}^{-1}$, $f = 0.21 \text{ mm}$

Slika 2: Odrezki po struženju 100Cr6 (kaljeno, 62 HRC), SEM, $v_c = 100 \text{ m min}^{-1}$, $f = 0.21 \text{ mm}$

the strain hardening.⁴ The materials sensitive to a formation of a shear-localized chip can be characterized with poor thermal properties (titanium alloys, maraging steels) and a limited ductility (hardened steels).⁵

A proper understanding of the material-removal mechanisms taking place during hard cutting is essential for a process evaluation. An analysis of the work area is necessary to describe the chip generation in hardened materials. Depending on the cutting parameters and workpiece material properties, cutting may either lead to continuous or discontinuous chip formation.^{2,4,7} Continuous chips are formed during turning conventional soft steels (**Figure 3** – a decrease in the flow stress due to the thermal softening associated with an increase in the strain is less than the associated strain hardening⁴), while hard turning can lead to a formation of segmented chips. **Figures 1** and **2** illustrate a segmented chip during turning the hardened steel 100Cr6. **Figure 2** shows that the plastic deformation inside the segment is low and the material in this area stays nearly untouched. Deformation processes are concentrated in the shear zone, tool-chip contact and tool-workpiece contact. On the other hand, the formation of a continuous chip leads to a more homogenous dissipation of deformation processes across the whole chip (**Figure 3**).

It was found that the total energies entering the cutting processes of conventional and hard turning (derived from the cutting speed and tangential component of the cutting force) are nearly the same.^{8,9} The difference can

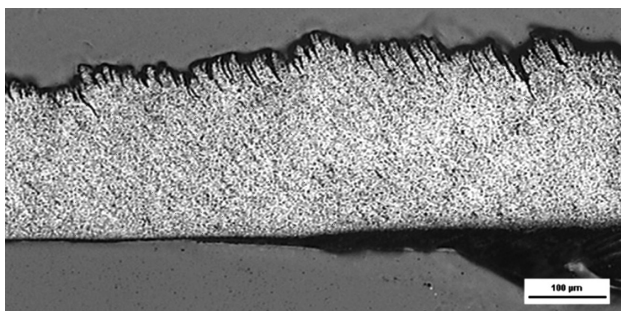


Figure 3: Chips after turning the 100Cr6 (annealed), SEM, $v_c = 100 \text{ m min}^{-1}$, $f = 0.21 \text{ mm}$

Slika 3: Odrezki po struženju 100Cr6 (žarjeno), SEM, $v_c = 100 \text{ m min}^{-1}$, $f = 0.21 \text{ mm}$

be found in the specific character related to the dissipation of this energy. An evaluation of the real intensity of deformation processes should be carried out with respect to the specific character of the chip formation. Intensity of deformation processes can be evaluated from the macroscopic point of view through metallographic observations. This conventional approach allows a calculation of the conventional parameters based on the measurements of chip thickness, undeformed chip thickness and derived parameters (deformation angle, chip speed, chip deformation and others). In this way, the average intensity of deformation processes in the cutting zone (across the whole chip) can be investigated.^{5,8}

An investigation of the real intensity of deformation processes related to the specific cutting zones is quite difficult and can be realized through acoustic emission (AE). The AE non-destructive technique is based on a detection and conversion of these high-frequency elastic waves to electrical signals. The major AE sources^{10,11} in a metal-cutting process are:

- deformation and fracture of work materials in the shear zone, tool-chip and tool-workpiece contacts;
- deformation and fracture of the cutting tool;
- collision, entangling and breakage of chips.

The main advantage of using AE to monitor a machining operation is that the frequency range of an AE signal is much higher than that of the machine vibrations and environmental noises, and does not interfere with the cutting operation.¹⁰ Due to its sensitivity to various contact areas and deformation regions during cutting, the AE signal is the basic tool for process monitoring.

Figures 2 and **3** show that the characters of deformation processes during the conventional soft and hard turnings differ. And so, the aim of this paper is to perform an analysis of the deformation processes in the cutting zone through the conventional metallographic observations and with the AE signal. Moreover, the differences between the conventional soft turning and hard turning should be investigated.

2 METALLOGRAPHIC OBSERVATIONS

The general aim of taking metallographic chip samples was to analyze the significant parameters of deformation processes in the cutting zone during hard turning and investigate the segmentation frequency in the chip (and comparing it with the frequency analysis from the accelerometer). The same analysis (except for the segmentation frequency) was carried out for soft steel with a view to comparing deformation processes in the cutting zone with respect to different properties of the machined material. The experimental setup and cutting conditions are listed in **Table 1**. **Figure 4** shows the chips, on which periodic cracks can be observed. These series of segments are measured all over the chip, and from more than 20 values the mean values are calculated. In the extensive cutting tests, the segmentation length and chip

thickness were statistically established. The parameters such as the chip ratio, the chip deformation, the chip speed, the shear speed, or the deformation angle were calculated. Moreover, the segmentation frequency could be evaluated. To obtain the segmentation frequency, the segmentation length had to be measured with a metallographic microscope and, knowing the cutting speed, the shear plane speed or the chip speed, and the frequency could be calculated.

Table 1: Experimental conditions during hard turning

Tabela 1: Eksperimentalni pogoji pri struženju

Cutting tool:	TiC reinforced Al ₂ O ₃ ceramic inserts DNGA150408 (TiN coating), rake angle $\gamma_n = -7^\circ$
Work material:	100Cr6 (hardened, 62 HRC and annealed, 27 HRC), external diameter of 56 mm, internal diameter of 40 mm, 125 mm long
Cutting condition:	$v_c = 25\text{--}250\text{ m min}^{-1}$, $f = 0.09\text{ mm}$, $a_p = 0.25\text{ mm}$ (constant), dry cutting
Machine tool:	CNC Lathe Hurco TM8

The chip thickness was measured with a light microscope

Intensity of a plastic deformation in the cutting zone can be expressed in terms of various parameters. Except for the chip ratio, there are parameters such as the degree of segmentation (G) or chip deformation (γ_{sh}) and other derived parameters such as the chip and shear speeds.

The measurement of the chip thickness was carried out with an optical microscope and through the measurement of the etched chips shown on **Figure 4**.

The measurement of the chip thickness (h_c) allows us to calculate the chip ratio (equation (1)) and the other related parameters such as the shear angle Φ_1 , the chip speed (v_{ch}), the shear speed (v_{sh}) and the chip deformation (γ_{sh}):

$$K = \frac{h_c}{h} \quad (1)$$

where h is the undeformed-chip thickness and h_c is the chip thickness. The deformation angle can be calculated through equation (2):

$$\text{tg } \Phi_1 = \frac{\cos \gamma_n}{K - \sin \gamma_n} \quad (2)$$

The chip speed and shear speed can be derived from the cutting speed and shear angle (equations (3) and (4)):

$$v_{ch} = v_c \frac{\sin \Phi_1}{\cos(\Phi_1 - \gamma_n)} \quad (3)$$

A chip deformation can be expressed in a similar way, through equation (5):

$$v_{sh} = v_c \frac{\cos \gamma_n}{\cos(\Phi_1 - \gamma_n)} \quad (4)$$

$$\gamma_{sh} = \frac{\cos \gamma_n}{\cos(\Phi_1 - \gamma_n) \cdot \sin \Phi_1} \quad (5)$$

A degree of segmentation is calculated through equation (6) and illustrated in **Figures 4** and **5**:

$$G = \frac{h_c - h_0}{h_c} \quad (6)$$

Figure 6 illustrates that the chip thickness during turning hardened steel is much lower than that during turning annealed steel. The metallographic observations verify the previous investigations performed under similar conditions.^{12–14} The formation of the segments during turning hardened steel causes an elongation and a decrease in the chip thickness. As a result of the formation of thin and long chips, the chip ratio is smaller than 1, contrary to the turning of annealed steel (thick and short continuous chips causing the chip ratio to be

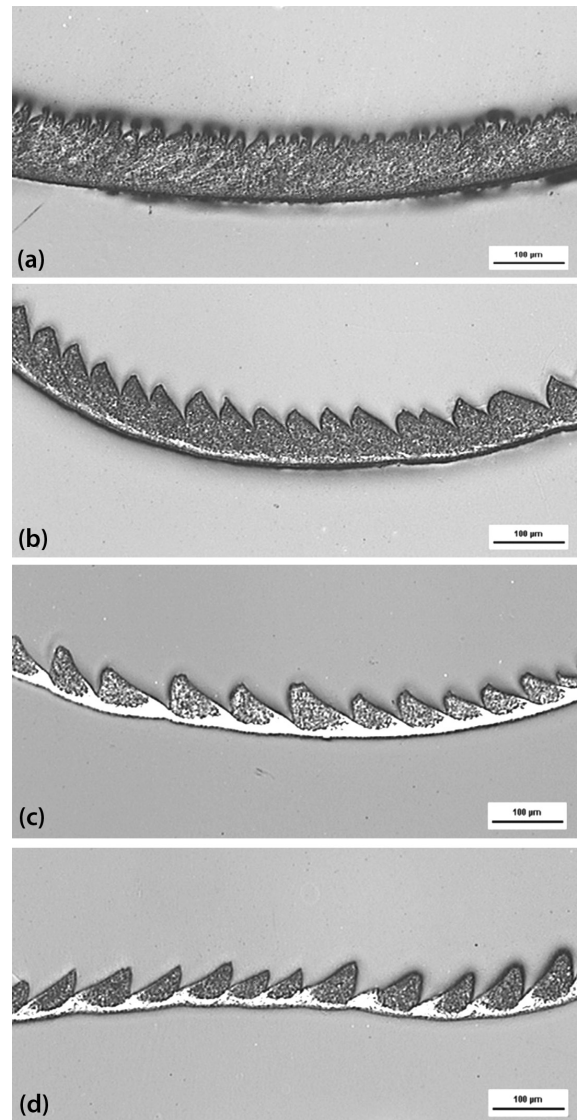


Figure 4: Chips after hard turning: a) $v_c = 25\text{ m min}^{-1}$, $f = 0.09\text{ mm}$, b) $v_c = 50\text{ m min}^{-1}$, $f = 0.09\text{ mm}$, c) $v_c = 100\text{ m min}^{-1}$, $f = 0.09\text{ mm}$, d) $v_c = 200\text{ m min}^{-1}$, $f = 0.09\text{ mm}$

Slika 4: Odrezki po struženju: a) $v_c = 25\text{ m min}^{-1}$, $f = 0,09\text{ mm}$, b) $v_c = 50\text{ m min}^{-1}$, $f = 0,09\text{ mm}$, c) $v_c = 100\text{ m min}^{-1}$, $f = 0,09\text{ mm}$, d) $v_c = 200\text{ m min}^{-1}$, $f = 0,09\text{ mm}$

more than 1, **Figure 7**). The average intensity of plastic deformation expressed with the chip ratio is much lower during hard turning than during the turning of soft steel.

The low intensity of plastic deformation must be attributed, first of all, to the material inside the segment. The plastic deformation inside the segment is low and the material in this area stays untouched. Although the plastic deformation in the localized areas of the segmented chip is extremely high (white areas), the total deformation of the segmented chip is much lower than for a continuous chip (during turning the annealed steel), as seen on **Figure 8**. On the other hand, the intensity of plastic deformation significantly changes with the cutting speed in the case of hard turning. The segmented chip becomes more continuous with a decreasing cutting speed. This aspect is verified with the degree of segmen-

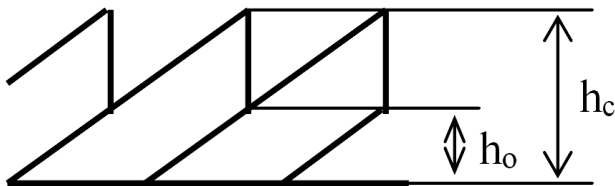


Figure 5: Illustration for a calculation of chip segmentation
Slika 5: Prikaz segmentacije odrezkov za izračun

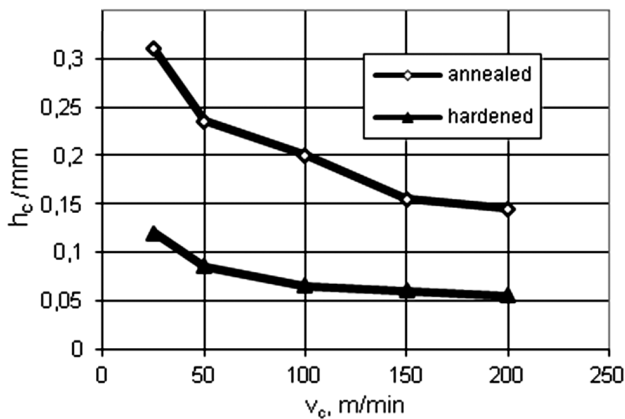


Figure 6: Influence of cutting speed on chip thickness
Slika 6: Vpliv hitrosti rezanja na debelino odrezka

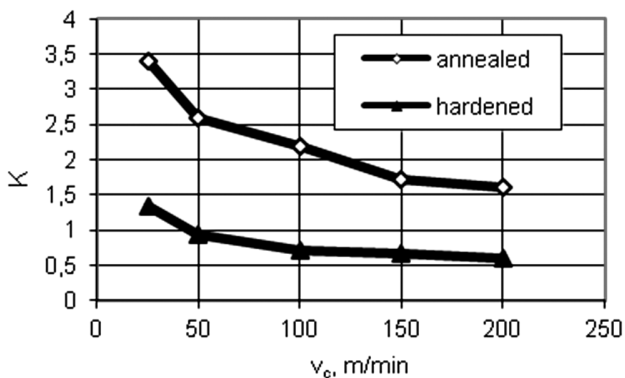


Figure 7: Influence of cutting speed on chip ratio
Slika 7: Vpliv hitrosti rezanja na razmerje odrezkov

tation illustrated in **Figure 9**. The continuous chip can be expressed as a segmented chip with the zero degree of segmentation. **Figure 9** illustrates that the degree of segmentation strongly decreases with a decreasing cutting speed. The specific character of the chip formation is related to the high shear angle, higher than the shear angle for turning annealed steel (**Figure 10**). The chip thickness, the chip ratio and the chip deformation increase with a decreasing cutting speed because the average intensity of plastic deformation increases (the chip becomes more and more continuous).

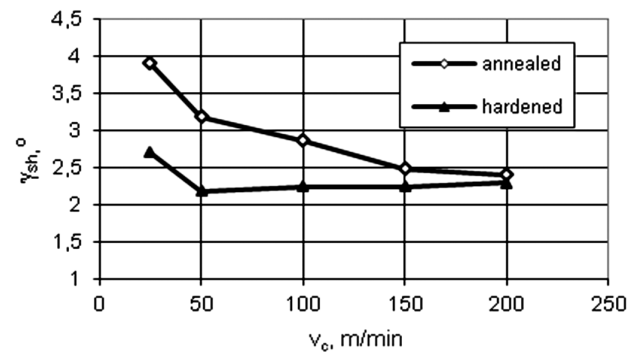


Figure 8: Influence of cutting speed on chip deformation
Slika 8: Vpliv hitrosti rezanja na deformacijo odrezkov

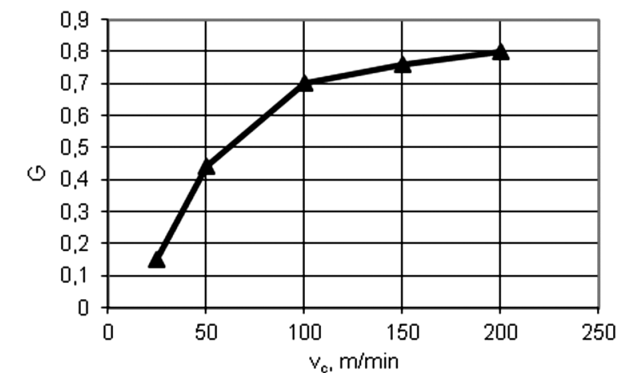


Figure 9: Influence of cutting speed on degree of segmentation
Slika 9: Vpliv hitrosti rezanja na stopnjo segmentacije

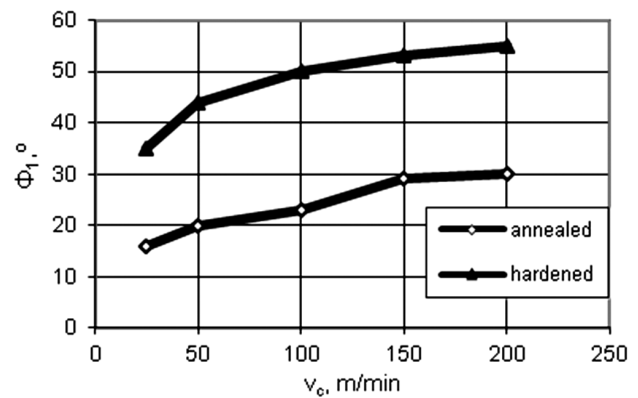


Figure 10: Influence of cutting speed on shear angle
Slika 10: Vpliv hitrosti rezanja na strižni kot

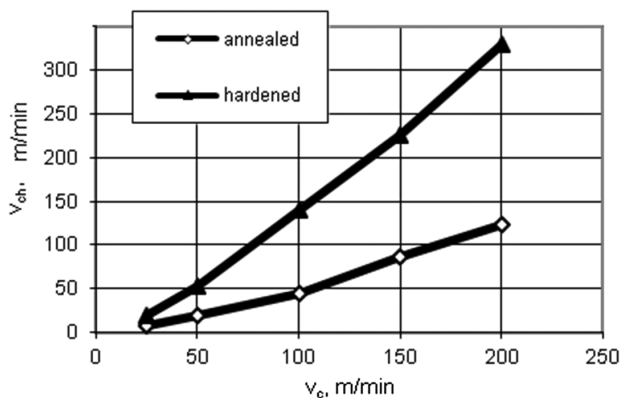


Figure 11: Influence of cutting speed on chip speed

Slika 11: Vpliv hitrosti rezanja na hitrost odrezka

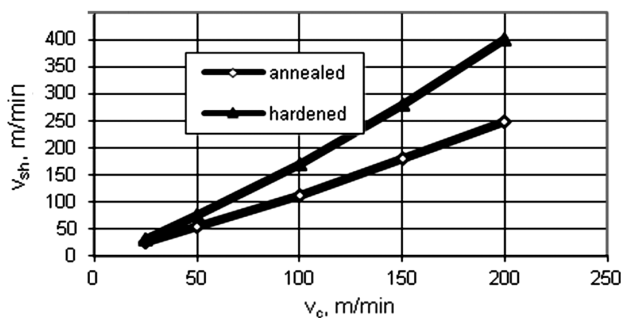


Figure 12: Influence of cutting speed on shear speed

Slika 12: Vpliv hitrosti rezanja na hitrost striženja

As a result of the formation of the thin and long chips (in the case of turning hardened steel) the shear speed and the chip speed are much higher than in the case of turning annealed steel (Figures 11 and 12). This aspect is attributed to the balance in the cutting zone between the incoming and outgoing volumes of the material. The increase in the chip ratio is strongly associated with a decrease in the chip speed.

It can be easily observed that the specific process of a chip segmentation leads to the thinning of the plastically deformed region as the chip moves up the tool face.^{12,13} The significance of the thinning of the plastically deformed region as the chip moves up the tool face is that this gives rise to a chip ratio less than one. This is usually the case when hard steel is turned with a negative rake tool. An important consequence is that the chip speed will be greater than the cutting speed and the shear angle will be greater than 45° .

3 EXPERIMENTAL RESULTS

The term segmented chip is often used to describe all of the cyclic types. This is unfortunate since these types of chips are distinctly different. For example, the cycle frequency for a wavy chip is typically about 100 Hz, while the one for a segmented chip is by 2 to 4 orders of magnitude greater.¹³⁻¹⁵ Dynamic forces that fluctuate at a frequency over 10 kHz are difficult to measure.

A conventional piezoelectric dynamometer limits the frequency response to about 3.5 kHz. However, an estimation of the relative changes in the force components and the frequency of force fluctuation may be obtained by using wire-resistance strain gauges¹⁵ or accelerometers. A conventional accelerometer limits the frequency response to about 20 kHz (special accelerometers limit the frequency response to about 50 kHz).

On the other hand, acoustic-emission techniques allow us to investigate the processes that fluctuate at a frequency over several MHz. AE signals can be classified into two types,¹⁶ as either continuous-type AE signals or burst-type AE signals. Continuous signals are associated with the shearing in the primary zone and the wear on the tool flank, while the burst type signals are observed during a crack growth in a material, tool, material fracture or chip breakage.

Apart from the conventional process monitoring, AE can be applied to an analysis of a chip form and a chip flow. The specific character of an AE signal can be observed under the specific cutting conditions related to a specific chip formation. Hard turning represents the case of a specific character of deformation processes mixed with a fracture of a machined material. There is a strong relaxation character of the related AE signal during hard turning. Uehara¹⁷ reported on remarkable patterns of the AE related to the segmented-chip formation. The AE signals accompanying the formation of a segmented chip exhibit remarkable patterns; the tool side signal shows a periodic bursting. The amplitude of AE varies correspondingly to the periodic change of the cutting force.

The elastic waves arising from different locations in the cutting zone can be detected through an AE system.^{10,17} The friction between the tool and the workpiece in the primary shear zone generates a continuous AE signal (during a formation of a continuous chip), providing comprehensive information on the cutting process. On the other hand, the chip formation during machining hardened steel allows us to work out the conditions for crack initiation and propagation. The surfaces that need to be machined are not perfectly smooth but rough and composed of microscopic ridges, cracks, voids, etc. Machining hardened materials using high compressive stress creates a subsurface material flow leading to the formation of cracks in the free surface. Strong elastic waves related to the crack formation during the segmented-chip formation can be detected through the AE systems, being inherent to the AE signals and related to the deformation processes in the cutting zone. The character of the AE signals during hard turning is complicated because mixed types of AE signals are generated in different zones. The aim of this experimental study is to analyze these aspects.

The experimental setup is shown in Figures 13 and 14. Commercial piezoelectric AE sensors (D9241A – the frequency range of 20 kHz to 180 kHz, WD – the frequency range of 100 kHz to 1000 kHz) by Physical

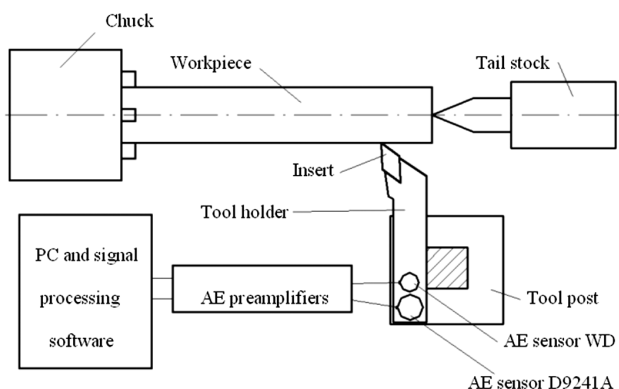


Figure 13: Schematic of experimental setup
 Slika 13: Shematski prikaz eksperimentalnega sestava

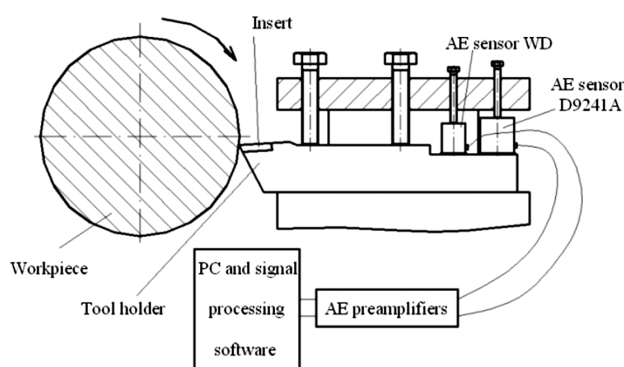


Figure 14: Detail of sensor placement
 Slika 14: Detajl namestitve senzorjev

Acoustics Corporation (PSC) were mounted on the top of the tool holder. To maintain a good propagation of the signals from the tool holder to the sensor, a semi-solid, high-vacuum grease was used. During the experiment, the AE signals were amplified, high passed at 20 kHz, low passed at 1000 kHz, and then sent through a pre-amplifier, at a gain of 40 dB, to the signal-processing software package. All the cutting tests were performed on a CNC lathe. The signals were real-time sampled, amplified, digitized and then fed to the signal processing unit. The AE signals were post-processed using AEwin.

3.1 Frequency analysis

When analyzing AE signals during hard turning, the segmentation frequency must be taken into consideration in relation to the frequency response of the applied AE sensors. Two sensors with different frequency ranges were applied. While the D9241A AE sensor allows us to analyze low frequencies (from 20 kHz), the low frequency limit of the WD AE sensor is 100 kHz.

The mean cycle frequency of the chip segmentation can be determined by dividing the speed of the chip v_{ch} by the mean spacing of the points of the maximum chip thickness p_c (the segment length in Figure 1) using equation 7:¹³

$$\text{segmentation frequency} = \frac{v_{ch}}{p_c} \quad (7)$$

To obtain the segmentation frequency, the segmentation length had to be measured with the metallographic microscope. Figure 4 illustrates that the segment length is not constant; it varies and so the segmentation frequency is not established as an exact value, but should be determined within a certain interval. As shown on Figure 15, the calculated segmentation frequencies lie in the frequency range of 10 kHz to 85 kHz. The verification of these frequencies can be performed through an application of the D9241A AE sensor, as the calculated frequencies are in the frequency range (or close to the low frequency limit at the low cutting speed) of this sensor.

An AE analysis could be limited under specific conditions because it could be difficult to find a relation between a physical process and the character of the AE signals. Because of this, many parameters of the AE signals implemented into the software package, such as the amplitude, the number of hits and counts, the signal strength, the energy, the average frequency and others could be analyzed. These parameters are derived from an AE wave with relation to the threshold value and they do not have to reflect the dynamic character of the process in real time. For example, Figure 15 illustrates that the segmentation frequency increases with the cutting speed. Figure 16 shows the relaxing and periodic character of the signal at different cutting speeds.

The time period between two consecutive amplitudes of an AE signal should reflect the segmentation frequency and should change in relation to different frequencies under different cutting conditions. Figure 16 illustrates that the time period between two consecutive pulses of an AE signal does not change and stays nearly constant. This is associated with the AE waveform transformation. The transformation of an AE waveform is compounded by the sensor response. When a resonant sensor is excited by a broadband transient pulse, it rings like a bell at

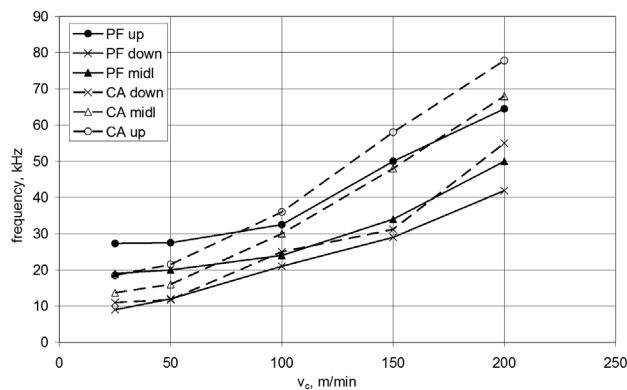


Figure 15: Influence of cutting speed on the peak frequency (PF) of the D9241A sensor and calculated segmentation frequency (CA)
 Slika 15: Vpliv hitrosti rezanja na maksimalno frekvenco (PF) senzorja D9241A in izračunana frekvenca segmentacije (CA)

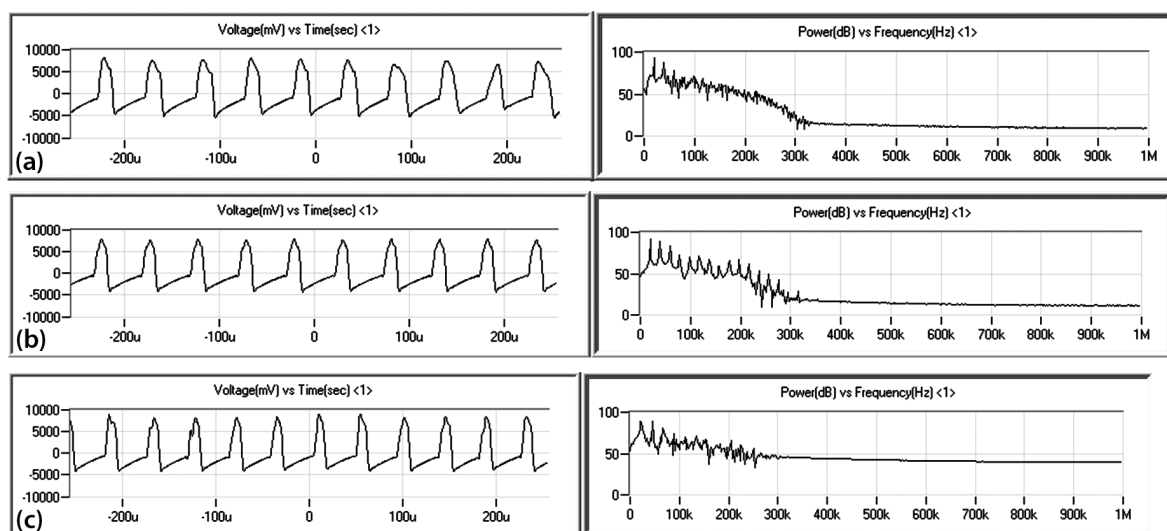


Figure 16: Signal of AE and its FFT spectrum for the 9241A sensor, hard turning: a) $v_c = 25 \text{ m min}^{-1}$, b) $v_c = 100 \text{ m min}^{-1}$, c) $v_c = 200 \text{ m min}^{-1}$
Slika 16: Signal AE in njegov FFT-spekter za senzor 9241A, struženje: a) $v_c = 25 \text{ m min}^{-1}$, b) $v_c = 100 \text{ m min}^{-1}$, c) $v_c = 200 \text{ m min}^{-1}$

its own frequency of oscillation. Therefore, the electrical signal at the sensor output is the product of this ringing, thus compounding the effects of multiple paths and multiple wave modes, with which the wave travels from the source to the sensor. The transformation of the AE waveform leads to a mismatch between the real dynamics of the signal and the derived AE parameters.

For example, the average frequency of the AE signal is determined as the average frequency over the entire AE hit and is derived from the AE-signal duration and the number of the counts (a count is a signal excursion over the AE threshold). This derived parameter (during this experiment) is in the range of 21 kHz to 24 kHz (for the D9241A sensor) and does not match the calculated values of the segmentation frequency in **Figure 16**. On the other hand, the applied AE system has the capability of calculating and processing the frequency-derived AE features in real time. Up to six frequency-based features can be processed by the AE system. Each of these features requires that a real time FFT is performed on the received AE-hit waveform. Except for four partial power frequency features, including the AE frequency features, they include frequency centroid and peak frequency (PF). The investigations into the centroid and peak frequency show that only the peak frequency (illustrated in **Figure 15**) matches the calculated values. The peak frequency is defined as a point in the power spectrum, at which the peak magnitude occurs. A real-time FFT (fast Fourier transformation) is performed on the waveform associated with the AE hit. The frequency that contains the largest magnitude is reported. Like the calculated values, the peak frequencies do not represent the exact values, but the AE Win software also processes this feature as an interval. **Figure 16** shows a good correlation between the peak frequencies and the calculated frequencies as an evidence of the AE system's capability

of truly reflecting the specific processes in the cutting zone during hard turning.

3.2 Intensity of deformation processes

It should be established that the AE sensors' responses depend on the frequency range of the applied sensor and the cutting speed. **Figures 16** and **17** illustrate the AE signals for different cutting speeds and the related FFT spectrums. It can be easily observed that the course of an AE signal (for the low-frequency sensor D9241A) reflects the relaxation character of the chip formation. The relaxation course of the signal is related to the relaxation process of the stress ahead of the cutting edge and the crack propagation in the shear region. According to the theory of the crack propagation and segment formation, the change in the amplitude of AE indicates a change in the sliding velocity during the tool-chip interface. Many pulse-like signals are observed, corresponding to the periodic fluctuation (the relaxation character) of the cutting process. The signal level of the AE between these pulses is quite small. During the segmented chip formation, the chip slides over the rake face with a varying speed corresponding to the period of the fracture in the shear plane.

Figure 16 shows the periodic peaks in the FFT spectrum. This character of the FFT spectrum confirms the dominant periodic character of the recorded signal and an ability of the D9241A AE sensor (the frequency range of 20 kHz to 180 kHz) to detect the periodic process typical for a segmented-chip formation. The segmentation frequencies of the investigated cutting speeds lie in the frequency range of the D9241A AE sensor (or close to the low-frequency limit). On the other hand, **Figure 17** illustrates that these peaks are missing during the formation of a continuous chip. Moreover, the excited amplitudes in the FFT spectrum during hard turning are

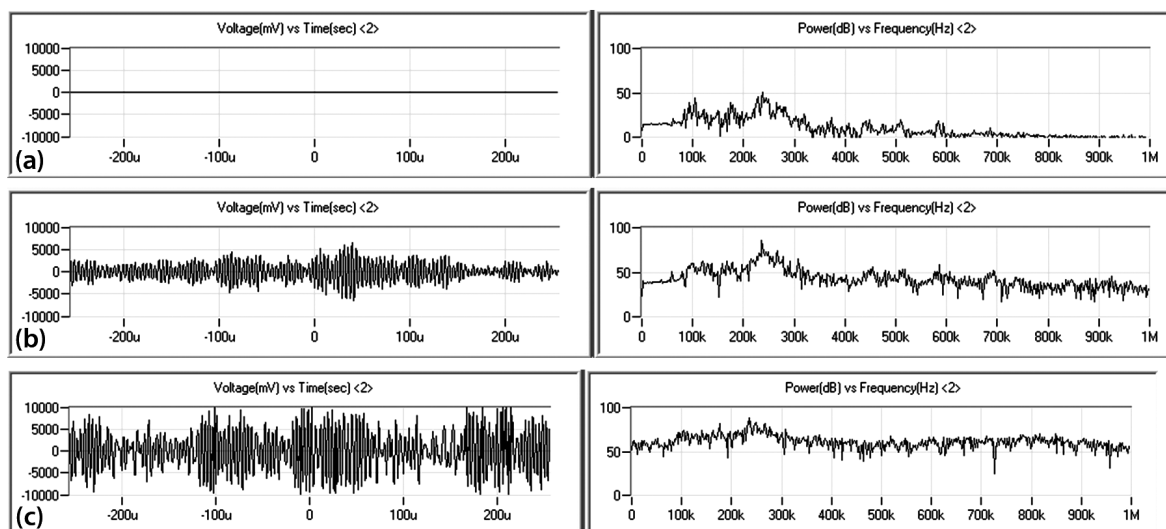


Figure 17: Signal of AE and its FFT spectrum for the WD sensor, hard turning
 Slika 17: Signal AE in njegov FFT-spekter za WD-senzor, struženje

significantly higher (above 50 dB, up to the 200 kHz frequency) in comparison with those occurring during the formation of continuous chips. It should be stated that the amplitudes of the AE signals, together with the amplitudes in the FFT spectrums, are nearly on the same level for all the cutting speeds. This indicates that the low-frequency AE sensor D9241A can be applied when making dynamic analyses (frequency responses) of hard turning, but this sensor is not sensitive to the variation of the deformation-process intensity in the cutting zone.

Considering the AE WD sensor (the frequency range of 100 kHz to 1000 kHz), all the segmentation frequencies lie outside the frequency range of this sensor and the periodic character of the AE signal is missing. The FFT spectrum of the AE signal for the WD sensor is

without the periodic peaks in this spectrum (Figure 17) as well as FFT spectrum in the case of turning annealing steel (Figure 18).

It was reported in the previous sections that AE signals can be classified into two types as either continuous-type AE signals or burst-type AE signals. Continuous signals are associated with the shearing in the primary zone, in the tool-chip and tool-workpiece contacts (Figure 19). These processes can be investigated and detected with the WD AE sensor, because the signals related to the chip segmentation (the crack propagation) are out of the segmentation-frequency range. Figure 17 shows that the amplitude of the AE signal for the WD sensor increases with the cutting speed. This aspect is associated with the increasing intensity of the friction

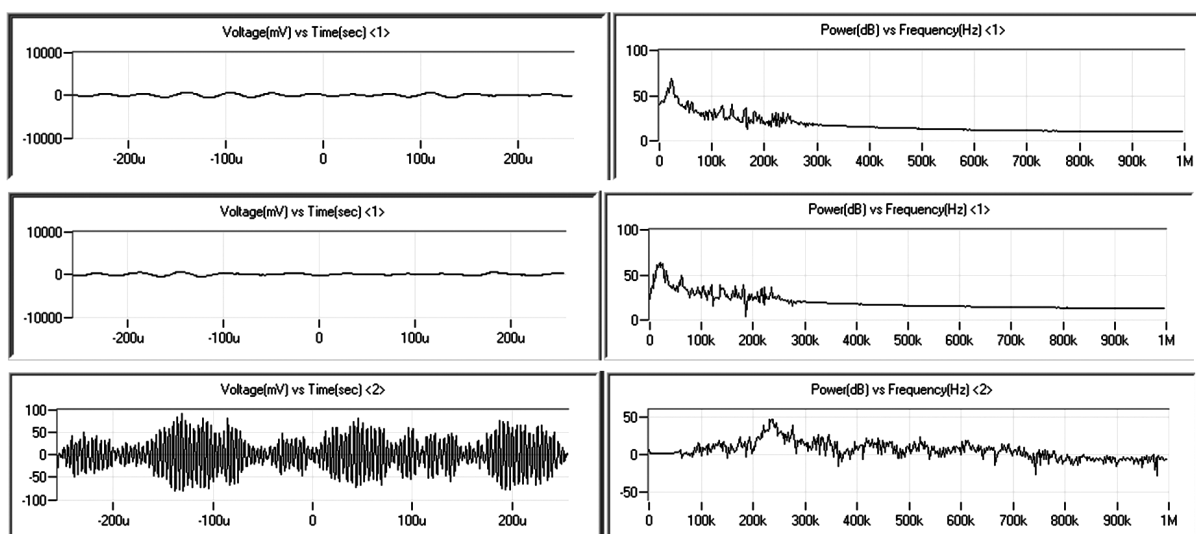


Figure 18: Signal of AE and its FFT spectrum, turning of annealed steel: a) $v_c = 25 \text{ m min}^{-1}$, 9241A sensor, b) $v_c = 100 \text{ m min}^{-1}$, 9241A sensor, c) $v_c = 200 \text{ m min}^{-1}$, WD sensor

Slika 18: Signal AE in njegov FFT-spekter, struženje žarjenega jekla: a) $v_c = 25 \text{ m min}^{-1}$, 9241A senzor, b) $v_c = 100 \text{ m min}^{-1}$, 9241A senzor, c) $v_c = 200 \text{ m min}^{-1}$, WD senzor

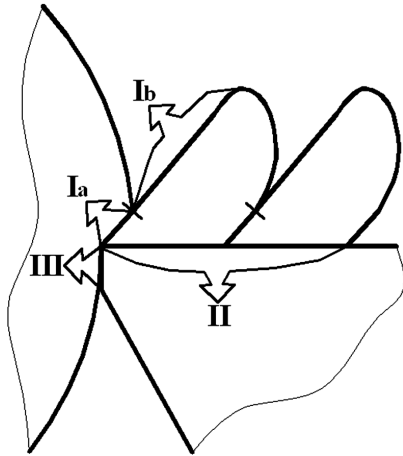


Figure 19: Cutting zone for hard cutting: Ia) microcracked and plastically deformed shear zone, Ib) cracked region, II) tool-chip contact, III) tool-workpiece contact

Slika 19: Cona odrezovanja pri rezanju: Ia) plastično deformirano strižno področje z mikrorazpokami, Ib) razpokano področje, II) stik orodje-odrezek, III) stik orodje-obdelovanec

processes in the cutting zone in relation to the increasing chip and shear speeds. Moreover, the amplitudes of the related frequencies in the FFT spectrum are excited above 50 dB, across the whole frequency range and at the cutting speed of 200 m min⁻¹, while the amplitudes in the frequency spectrum at the cutting speed of 25 m min⁻¹ are lower (Figure 17).

An application of the D9241A sensor is limited for these analyses. The burst-type AE signal (related to the crack propagation) superposes with the signal from the tool-chip and tool-workpiece interface and so it causes the difficulties in the investigation of the processes in these regions. The segmentation frequencies lie in the frequency range of the D9241A sensor. These frequencies are associated with the crack formation and its propagation in the shear zone. The signal associated with a crack formation and its prolongation in the shear zone is very strong (the amplitude of the AE signals for all the cutting speeds is on the maximum level of 100 dB) generating a massive low-frequency noise. This noise negatively influences the detection of the friction process

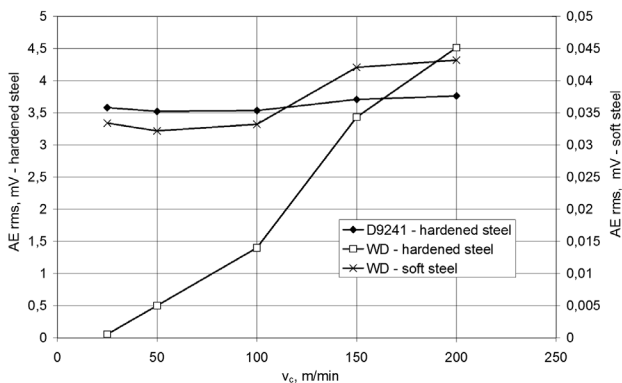


Figure 20: Influence of cutting speed on RMS values of AE
Slika 20: Vpliv hitrosti rezanja na RMS-vrednosti AE

in the shear zone, the tool-chip and tool-workpiece contacts (Figure 19). The AE signals recorded by the D9241A sensor are not sensitive to the friction processes in the cutting zone. Figures 20, 21 and 22 show that the RMS value, the signal strength and the absolute energy of the AE signal do not vary significantly with the increasing cutting speed. (The signal strength is defined as the integral of the rectified voltage signal over the duration of the AE waveform packet. The absolute energy is a true energy measure of the AE hit.)

On the other hand, the frequency range of the WD sensor lies above the segmentation frequencies and so the low-frequency limit of 100 kHz of the WD sensor represents a high-pass filter. The RMS values, the strength and the absolute energy of the AE signal increase with the increasing cutting speed (Figures 20, 21 and 22). This aspect is associated with an increasing intensity of the deformation processes in the cutting zone. These processes are dissipated to the narrow white areas in the shear zone (the white area is caused by the plastic deformation in this zone, contrary to the crack formation in the area without an occurrence of a structure transformation) as well as to the tool-chip and tool-workpiece contacts. The increase of the values in Figures 20, 21 and 22 cannot be attributed to the tool wear because all the tests were carried out in the normal phase of the tool wear (its VB being from 0.1 mm to

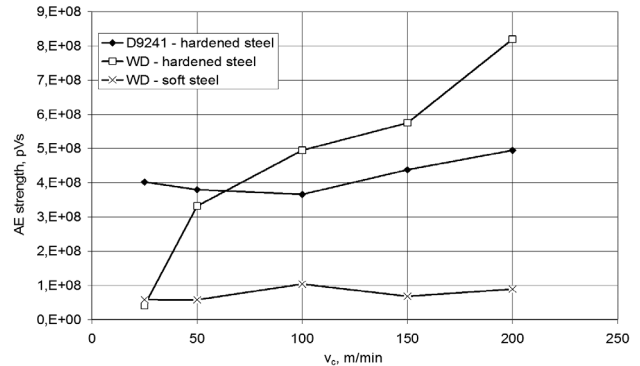


Figure 21: Influence of cutting speed on AE signal strength
Slika 21: Vpliv hitrosti rezanja na moč AE-signalna

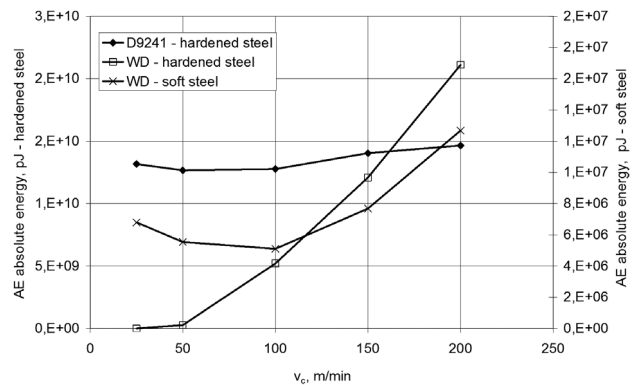


Figure 22: Influence of cutting speed on absolute energy of AE
Slika 22: Vpliv hitrosti rezanja na absolutno energijo AE

0.12 mm). The increasing intensity of deformation processes is attributed to the following aspects:

the increasing chip segmentation with the increasing cutting speed; a more intensive thinning of the micro-cracked region (the plastically deformed shear zone) as the chip moves up the face of the tool;

- the increasing non-homogeneity in the stress and temperature distribution in the cutting zone with the increasing cutting speed, together with the increasing chip and shear speeds;
- the temperature in the cutting zone increases with the increased cutting speed⁸ (forming suitable conditions for the processes of plastic deformation and the related structure transformation and reducing the zones of an undeformed chip).

The sensitivity of the AE signals concerning the intensity of the real-deformation processes in the cutting zone can be illustrated through a comparison of the AE signal and FFT spectrums during conventional (annealed steel) turning and hard turning. The analytic approach shows that the chip deformation and chip ratio are higher for the conventional continuous chips (**Figures 7 and 8**), but the amplitude of the AE signals and the excited amplitudes of the FFT spectrums in **Figure 18** are significantly lower. While the amplitudes of the AE signal during hard turning oscillate between ± 10000 mV, the formation of a continuous chip leads to an oscillation on the scale of ± 100 mV. Moreover, the excited amplitudes of the FFT spectrum in **Figure 18** are close to zero (except for the resonance frequency represented by the maximum amplitude in the spectrum), while, in contrast, those amplitudes excited above 50 dB cover the whole frequency spectrum during hard turning (**Figure 17**). Some other derived parameters such as the RMS value of the AE signal, the signal strength and the absolute energy are closely associated with the emission signals, correlating with the amplitude range of the responded emission waves. **Figures 20, 21 and 22** illustrate that all the values are significantly lower during the formation of conventional chips.

The metallographic and experimental studies give contradictory results because of their different methodologies. For example, the values of the chip ratio or the chip deformation for the hard-turning process in **Figures 7 and 8** decrease with the increasing cutting speed. This indicates a decreasing intensity of deformation processes in the cutting zone. However, **Figures 17, 18, 21 and 22** show that the absolute energy, the signal strength and the amplitudes of the AE signals increase with the increasing cutting speeds.

The conventional analytical approach does not facilitate an evaluation of the real intensity of deformation processes in the specific zones of the cutting process. This approach takes the whole chip into the consideration. The calculated values do not reflect the non-homogeneity of deformation processes during hard cutting, but provide information about the average value across the whole chip. On the other hand, the experi-

mental study (based on AE) can identify the real intensity of this specific process.

4 CONCLUSIONS

The findings of this study show that the AE signals can be used to monitor the dynamic character and intensity of plastic deformation in the cutting zone during hard turning in the following ways:

- metallographic analyses and the related calculations allow an analysis of the real intensity of deformation processes during the formation of conventional continuous chips, but this approach is less sensitive to the identification of the specific-character chip formation during hard turning;
- experimental analysis of the chip formation during hard turning should be investigated with respect to the specific dynamic character of the cutting process and the related frequencies;
- burst type of the AE signal is associated with a crack propagation in the shear zone because of the relaxing character of the chip formation and the related segmentation frequencies;
- analysis of the chip segmentation requires a match of the segmentation frequency and the frequency range of the applied AE sensor;
- continuous type of the AE signals is associated with the plastic deformation in the cutting zone related to the plastic deformation in the shear zone, the tool-chip and tool-workpiece sliding contacts;
- continuous type of the AE signal is more sensitive to the real intensity of deformation processes during hard turning, contrary to the metallographic analyses and the calculated parameters.

The dynamic character of a cutting process in hard turning and the specific character of a chip formation significantly affect the parameters such as the shear and chip speeds, the friction processes in the cutting zone, the related heat generation and high temperatures in this zone. These parameters have an impact on the surface quality represented by the residual stresses, surface hardness, structural changes and other attributes. And so, the studies about the dynamic character of the hard-turning process should be carried out.

Acknowledgement

This paper was supported by the Students Grant Competition of VSB-TU Ostrava, "SP2012/68 Effective machining of progressive materials and integrity surface evaluation", and also by the VEGA agency.

5 REFERENCES

- ¹ G. Bartarya, S. K. Choudhury, State of the art in hard turning, International Journal of Machine Tools and Manufacture, 53 (2012) 1, 1–14

- ² D. Kramar, J. Kopač, High Pressure Cooling in the Machining of Hard-to-Machine Materials, *Journal of Mechanical Engineering*, 55 (2009) 11, 685–694
- ³ R. F. Recht, Catastrophic Thermoplastic Shear, *Trans ASME*, 86 (1964), 189–193
- ⁴ K. Nakayama, M. Arai, T. Kanda, Machining Characteristics of Hardened Steels, *CIRP Annals*, 37 (1988) 1, 89–92
- ⁵ M. A. Elbestawi, A. K. Srivastava, T. I. El-Wardany, A Model for Chip Formation during Machining of Hardened Steel, *CIRP Annals*, 45 (1996) 1, 71–76
- ⁶ R. Komanduri, R. H. Brown, On the Mechanics of Chip Segmentation in Machining, *J. of Eng. for Ind. Trans. ASME*, 103 (1981), 33–51
- ⁷ G. Poulachon, A. Moisan, I. S. Jawahir, On Modeling the Influence of Thermo – Mechanical Behavior in Chip Formation during Hard Turning of 100Cr6 Bearing Steel, *CIRP Annals*, 50 (2001), 31–36
- ⁸ M. Neslušan, Turning of Hardened Steels, 1st ed., Edis Žilina, Žilina 2009, 245
- ⁹ M. Neslušan, R. Čep, B. Barišič, Chip formation analysis during hard turning, *Strojarstvo*, 50 (2008), 337–347
- ¹⁰ D. A. Dornfeld, Acoustic emission in monitoring and analysis in manufacturing, *Proceedings of AE Monitoring, Anal. Manuf.*, 14 (1984), 124
- ¹¹ D. A. Dornfeld, Manufacturing process monitoring and analysis using acoustic emission, *Journal of Acoustic Emission*, 4 (1985), 123–126
- ¹² G. Poulachon, A. Moisan, Contribution to the Study of the Cutting Mechanism during High Speed Machining of Hardened Steel, *CIRP Annals*, 47 (1998), 73–76
- ¹³ M. C. Shaw, A. Vyas, The Mechanism of Chip Formation with Hard Turning Steel, *CIRP Annals*, 47 (1998) 1, 77–82
- ¹⁴ M. C. Shaw, A. Vyas, Mechanics of Saw-Tooth Chip Formation in Metal Cutting, *ASME Journal of Manufacturing Science and Engineering*, 121 (1999), 163–172
- ¹⁵ B. Lindenberg, B. Lindstroem, Measurement of the Segmentation Frequency in the Chip Formation Process, *CIRP Annals*, 32 (1983) 1, 17–20
- ¹⁶ I. Inasaki, Application of acoustic emission sensor for monitoring machining processes, *Ultrasonics*, 36 (1998), 273–281
- ¹⁷ K. Uehara, Identification of Chip Formation Mechanism through Acoustic Emission Measurements, *CIRP Annals*, 33 (1974), 71–74